Structural and Conformational Requirements for Human Calcitonin Activity: Design, Synthesis, and Study of Lactam-Bridged Analogues

Afrodite Kapurniotu[1] and John W. Taylor*

Rutgers University, Department of Chemistry, P.O. Box 939, Piscataway, New Jersey 08855-0939

Received August 31, 1994[⊗]

The conformational and pharmacological effects of the introduction of conformational constraints in the form of $i-(i+4)$ lactam-bridges in the potential amphiphilic α-helical region (8-21) of human calcitonin (hCT) were studied. The following three cyclic hCT analogues were synthesized: *cyclo*[17,21]-[Lys[17],Asp[21]]hCT (**1**), *cyclo*[17,21]-[Asp[17],Lys[21]]hCT (**2**) and *cyclo*[10,14]-[Lys[10],-Asp[14]]hCT (**3**). For their syntheses, solid-phase methodology was used in combination with either direct side chain to side chain cyclization on the solid support or a segment-condensation strategy. Circular dichroism studies in aqueous buffer, pH 7.0, indicated that the conformational effects were different for each lactam bridge introduced. Significant induction of α-helical structure was observed only for peptide **3**. In contrast, peptide **1** and hCT had similar CD spectra, indicative of mixed disordered and β-sheet conformations, and peptide **2** had a weaker spectrum consistent with the formation of a more ordered but nonhelical structure. In rat brain receptor binding assays, peptide **2** showed a nearly 80-fold higher potency than hCT or peptides **1** and **3**. All three analogues stimulated adenylyl cyclase in the rat kidney membrane at 5-fold lower concentrations than hCT and with similar maximal effects. *In vivo* hypocalcemic assays, performed in mice by analysis of serum calcium levels 1 h after sc injection, indicated that peptide **2** had similar maximal effects to hCT and was 10-20 times more potent than hCT at doses giving half-maximal effects. In contrast, peptides **1** and **3** were not significantly more potent than hCT. Our findings indicate compatibility of all three lactam bridges and, most probably, also the amphiphilic α-helix, with the pharmacological activities of hCT. However, the properties of peptide **2** also suggest that another conformation, possibly a type I β-turn involving residues 17-20, may play an important role. A multistep mechanism of receptor recognition by hCT that might account for these results is discussed.

Introduction

Understanding the conformational features that determine the biological activities of short or medium-sized peptides is a complex task, mainly because their flexibility increases the likelihood that conformations not normally present in aqueous solution may be induced upon binding to cell-surface receptors, and detailed structures of ligand-receptor complexes are rarely available. Restriction of the peptide ligand flexibility, by incorporating cyclic structures that impose conformational constraints on segments of the peptide backbone, has been a successful approach toward the elucidation of the bioactive conformation of a number of peptides and the subsequent development of highly potent agonists or antagonists.[2]

A significant number of peptide hormones and neurotransmitters are observed to have the potential to form amphiphilic α-helical structures.[3,4] While the functional role of these structures is yet to be determined, they have long provided a rationale for the design of analogues that either test their importance or enhance their potency and/or specificity of action.[2-4] One approach to constraining the potential amphiphilic α-helical regions of biologically active peptides[5-10] or peptide models[11,12] is based on the incorporation of pairs of residues, such as Lys and Asp or Lys and Glu, spaced at positions i and $i+4$ in the linear sequence with their side chains lactam-bridged. In particular, incorporation of Lys^{i}, Asp^{i+4} and Asp^{i}, Lys^{i+4} lactam-bridged residue pairs has been demonstrated to result in helix stabilization in GRF[13] analogues,[5,6] in an NPY analogue,[7] in a PTHrP analogue,[10] and in model peptides.[12] Moreover, the above studies have led to the development of more potent and metabolically stable GRF analogues[5,6] and a potent PTHrP antagonist.[9]

Calcitonin is a peptide hormone of 32 residues that is in therapeutic use and is known mainly for its hypocalcemic effect and inhibition of bone resorption.[14,15] The primary structures of calcitonins from seven species show the following common features:[15] (i) a disulfide bridge between the cysteine residues 1 and 7; (ii) a highly conserved sequence in residues 3-7; and (iii) conserved amino acid residues in positions 1, 9, 28, and 32 (a prolinamide). A potential amphiphilic α-helical region in the central domain of the endogenous teleost (salmon and eel) calcitonins has also been predicted, and amino acid sequence differences in this region are linked to their higher potency compared to mammalian calcitonins.[16,17] Nevertheless, most commonly used hydrophobicity scales indicate that the amphiphilic character of an α-helical structure formed by residues 8-21 is preserved for all of the calcitonins, despite significant sequence variations.[18] The human calcitonin (hCT) structure is shown in Figure 1.

Structure-activity relationships of salmon calcitonin I (sCT), which exhibits the highest potency of the known native calcitonins and is about 50-fold more potent than hCT in hypocalcemic assays *in vivo*, have been the most extensively studied.[15-17,19-30] Early studies have demonstrated the requirement for the entire peptide structure for high agonist potency,[15,26] although single-residue deletions are well-tolerated in some positions.[20,29,30] In the proposed amphiphilic α-helical region (residues 8-21 or 8-22), Kaiser and co-

[⊗] Abstract published in *Advance ACS Abstracts,* January 1, 1995.

0022-2623/95/1838-0836$09.00/0

hCT: H-CGNLSTCMLGTYTQDFNKFHTFPQTAIGVGAP-amide

1: H-CGNLSTCMLGTYTQDFKKFHDFPQTAIGVGAP-amide

2: H-CGNLSTCMLGTYTQDFDKFHKFPQTAIGVGAP-amide

3: H-CGNLSTCMLKTYTDDFNKFHTFPQTAIGVGAP-amide

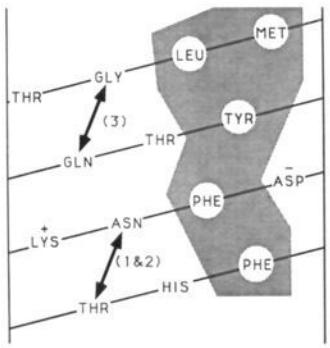

Figure 1. Structures of hCT and peptides **1**, **2**, and **3**. The linear amino acid sequences of each peptide are shown (top) together with a helical net diagram of hCT residues 8–21 (bottom). The positions of the lactam bridges in peptides **1**, **2**, and **3** are indicated by bold lines in the peptide sequences and bold double-headed arrows in the helical net diagram. The hydrophobic face of the amphiphilic helix is also indicated by shading.

workers[21–23] have adopted the approach of minimizing homology with the native sequence while maximizing amphiphilic character and helix-forming potential (according to Chou–Fasman[31] parameters) in order to test the structural requirements of this region. This study resulted in the design of two sCT analogues with multiple substitutions in the 8–22 region that showed similar pharmacological properties to the natural sCT and identified a conserved carboxylate side chain in residue position 15 as an important pharmacophore. Thus, evidence was provided that the model of an amphiphilic α-helical region in residues 8–22 is a useful guide to designing potent sCT activity. However, the importance of a specific carboxylate in this region supported earlier studies indicating that individual residues in this region are also important determinants of high potency. For example, replacement of the aromatic residues in positions 12, 16, and 19 of hCT with leucine residues, as is found in sCT, greatly enhances its *in vivo* potency.[27,28] Furthermore, other studies have suggested that conformational flexibility at Gly^{10}, and proposed long-range interactions within the calcitonin molecule that inhibit phospholipid binding by the amphiphilic α-helix, correlates better with pharmacological activity than does the α-helix content judged by circular dichroism (CD) spectropolarimetry.[24,25] Thus, the functional importance of the proposed amphiphilic helix in the central region of the calcitonins is presently unclear.

Three native calcitonins (salmon, porcine, and human) and an analogue ([$Asu^{1,7}$]-eel calcitonin) are used therapeutically,[32] mainly for the treatment of osteoporosis, Paget's disease, and hypercalcemia. To date, no calcitonin analogues have been described that are of significantly higher potency than native sCT. Also, the nonhuman calcitonins are frequently antigenic in humans, which could be one reason for the development of secondary resistance (i.e., desensitization) to the hormone.[32] There is, therefore, significant interest in the development of new, high-potency calcitonin analogues that maintain a close structural resemblance to native hCT.[27]. However, rational approaches to this goal require a better understanding of the conformational requirements of hCT for receptor binding and activation.

In order to provide a more stringent test than the earlier peptide models[21–23] of the requirements of the calcitonins for α-helical structure in residues 8–21, we now describe our initial studies on the effects of incorporating side-chain lactam bridges into this region of hCT. Three analogues have been compared, each incorporating a Lys^{i}, Asp^{i+4} or an Asp^{i}, Lys^{i+4} bridge onto the hydrophilic face of the proposed amphiphilic α-helix that was expected to stabilize the helical structure. For their syntheses, we used solid-phase methodology, combined either with the strategy of side-chain cyclization on the solid support[5] or with a segment-condensation strategy to incorporating the lactam-bridged structures. In the latter case, protected peptide segments were prepared separately by the oxime-resin cyclization method.[33,34] The conformational studies we now report, together with pharmacological assays for receptor binding, adenylyl cyclase activation, and *in vivo* hypocalcemic effects in mice, indicate that helix stabilization and pharmacological potencies are strongly dependent on both the position of the bridge and its specific structure, providing a significant contrast with similar studies of other hormones and model peptides.

Results

Peptide Design. Three hCT analogues with lactam bridges joining the side chains of residues Lys^{17} and Asp^{21} (**1**) or Asp^{17} and Lys^{21} (**2**) substituted for residues Asn^{17} and Thr^{21}, or residues Lys^{10} and Asp^{14} (**3**) substituted for residues Gly^{10} and Gln^{14}, were synthesized (Figure 1). These types of lactam-bridged structures were chosen before other possible structures on the basis of previous studies by CD and ^{1}H-NMR, indicating their α-helix stabilizing properties in peptide hormones[5–7,9] and model amphiphilic α-helical peptides.[11,12] To keep the hydrophobic face of the potential amphiphilic α-helix proposed for residues 8–21 intact (Figure 1), bridges were placed only in positions corresponding to the hydrophilic face of this helix. Also, charged residues were not chosen for substitution, in order to retain local and overall charge effects of the molecule. The lactam bridges in peptide **1** and peptide **2** were placed in the C-terminal half of the potential amphiphilic α-helix, whereas that in peptide **3** was placed in the N-terminal half of this structure. Together, this enabled us to compare the effects of lactam-bridged orientation (**1** and **2**) and location (**1** and **3**) on helix stabilization and biological activity.

Peptide Synthesis. The assembly of peptides **1** and **3** started with the separate synthesis of the fully protected and C-terminal free, lactam-bridged peptides N^{α}-Fmoc-*cyclo*^{17,21}-[Lys^{17},Asp^{21}]hCT(17–21)-OH (**6**) and N^{α}-Fmoc-*cyclo*^{10,14}-[Lys^{10},Asp^{14}]hCT(10–14)-OH (**7**), respectively. These syntheses were carried out using the oxime resin method[33] and applying a four-dimensional orthogonal protection scheme (Boc/Bzl/Fmoc/Al), as we described recently.[34] Cyclic pentapeptides **6** and **7** were then coupled in good yield (63% and 77%, respectively, based on **6** and **7**) to the appropriate protected peptidyl-

Scheme 1. Solid-Phase Synthesis of Peptide **1** by a Combined Stepwise and Segment-Condensation Approach

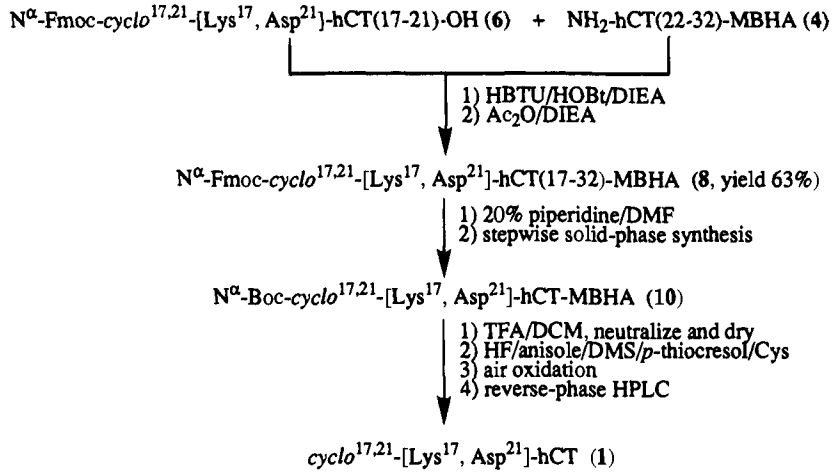

resins NH_2-(hCT(22−32))-MBHA (**4**) and NH_2-(hCT(15−32))-MBHA (**5**), which had been assembled by standard solid-phase methods. After capping unreacted sites and further elongation of the peptide chains on the MBHA resin, crude peptides **1** and **3** were obtained in their fully deprotected and reduced form by treatment of the peptidyl resin with HF/anisole/dimethyl sulfide/*p*-thiocresol (10/1/1/2, v/v/v/w). Cysteine (0.27 M) was added to this cleavage mixture in order to suppress a possible N-terminal thiazolidine formation,[35] a side reaction likely to occur during HF cleavage of peptides with N-terminal Cys and the Bom group for the side-chain protection of His. Formation of the 1 to 7 disulfide-bridge was performed by air oxidation of the crude products under high-dilution conditions, its completion followed by HPLC. Preparative reverse-phase HPLC purification gave dicyclic analogues **1** and **3** of high purity as shown by amino acid analysis, ion-spray MS, and analytical HPLC. This synthetic method is illustrated for peptide **1** in Scheme 1.

Peptide **2** was synthesized using the side chain to side chain cyclization strategy on solid support, as described by Felix et al.[5] The peptide chain was assembled on MBHA resin using the Boc/Bzl strategy with temporary Fmoc and OFm protection for the side chains of Lys^{21} and Asp^{17}, respectively. Because of the possibility of intermolecular lactam-bridge formation during the side chain to side chain cyclization,[36] peptidyl resin of relatively low substitution level (0.2 mmol/g of resin) was used for this synthetic strategy. The side chain to side chain cyclization was performed using HBTU in DMF, immediately following the assembly of Asp^{17}. Subsequent peptide chain elongation, followed by HF cleavage, disulfide-bridge formation, and preparative HPLC purification, gave peptide **2**. Structure and high purity were again confirmed by amino acid analysis, ion-spray MS, and analytical HPLC.

Difficulties were encountered in choosing the most effective method for the isolation of the desired products. All three crude peptides showed broad profiles on reverse-phase HPLC in combination with various CH_3CN/H_2O (containing 0.05% TFA) gradient systems, directly after the HF cleavage. However, treatment of crude products with reducing agents such as dithiothreitol or air-oxidation under high dilution conditions both resulted in much sharper HPLC profiles. Analytical HPLC of the purified reduced forms of the peptides

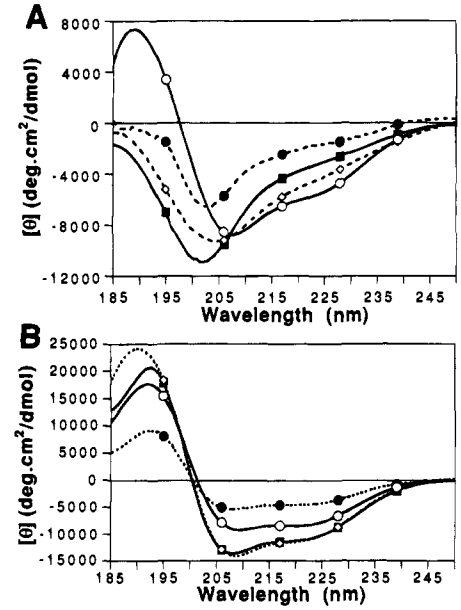

Figure 2. Circular dichroism spectra of peptides. Spectra were obtained at 25 °C from 50 μM solutions of hCT (■), peptide 1 (◇), peptide **2** (●), and peptide **3** (○) in (A) 10 mM sodium phosphate buffer, pH 7.0, and (B) aqueous buffer with 50% (v/v) TFE added.

also gave broad profiles. Susceptibility of the reduced forms of these peptides to intermolecular reactions through their free thiol groups, resulting in polymeric materials,[37] and/or interactions with the hydrophobic, reverse-phase material and/or coexistence of different conformers under these conditions might be possible reasons for the above profiles.[38] In addition, the Met^8 residue was shown to be very prone to oxidation, at least in acidic aqueous solutions. Therefore, for isolation of the desired peptides in good yields, one-step reverse-phase HPLC purification, after air-oxidation of the crude products, proved to be the most effective method. In contrast to their reduced forms, purified, dicyclic peptides or their solutions in 1 mM HCl (concentration range 200−500 μM) were stable for at least 6 months when stored at −20 °C.

Circular Dichroism Studies. Circular dichroism (CD) spectra of hCT and peptides **1**−**3** were first measured in aqueous 10 mM phosphate buffer (pH 7.0) at 25 °C and a concentration of 50 μM (Figure 2A). No concentration dependence of the CD spectra was observed in the concentration range between 5 and 50 μM,

Table 1. Quantitative Analysis of Circular Dichroism Spectra by Linear Combination of the Standard Peptide Spectra of Brahms and Brahms[39,40]

peptide[a]	secondary structure content (%)			
	α-helix	β-sheet	unordered	turn
hCT	7	27	57	8
peptide 1	10	27	54	9
peptide **2**	0	43	51	6
peptide **3**	16	32	45	7

[a] Peptide spectra were measured in 10 mM sodium phosphate buffer, pH 7.0, at 25 °C.

and hCT or other natural calcitonins have not been reported to aggregate in this concentration range. Therefore, the peptides were assumed to be monomolecular under the conditions studied.

A qualitative analysis of the spectra obtained for hCT, peptide **1**, and peptide **3** in the aqueous buffer is suggestive of small stepwise changes from a disordered structure (minimum at 198 nm) toward a more α-helical structure (minima at 208 and 222 nm), as anticipated from the incorporation of lactam bridges with demonstrated helix stabilizing properties. However, the crossover point for these spectra is about 207–209 nm, which is higher than expected for a pure helix-coil transition (202–203 nm), and the negative ellipticities observed for all three peptides are relatively small. These features indicate the likely presence of significant β-sheet structure.[39] Compared to the spectra of this group of peptides, the weaker CD spectrum of peptide **2** indicates a distinctly different nonhelical secondary structure content.

Quantitative linear regression analyses were performed to fit the spectra to (a) the standard spectra of Brahms and Brahms[39] (185–240 nm), which are derived from polypeptide models (Table 1), and (b) the basis set of spectra from Park and Fasman[40] (195–240 nm), which are derived from the CD spectra of globular proteins of known three-dimensional structure (Table 2). Both methods gave reasonably good fits to the CD spectra of hCT, peptide **1**, and peptide **3** using four basis spectra, and both methods confirmed the stepwise reduction in the amount of disordered structure in the series hCT > peptide **1** > peptide **3**. These analyses also indicated a small, stepwise increase in α-helix content in this series, and the presence of a significant structural component attributed to β-sheet (Brahms and Brahms, Table 1) or antiparallel β-sheet (Park and Fasman, Table 2). If the 16–17% overall α-helix content estimated for peptide **3** by both methods resides entirely in the peptide segment including residues 8–22, as suggested by secondary structure predictions[16] and ^{1}H-NMR in TFE–water (1/1) solution,[41] the α-helical content in this region of peptide **3**, the most helical peptide, is estimated to be no more than 33%.

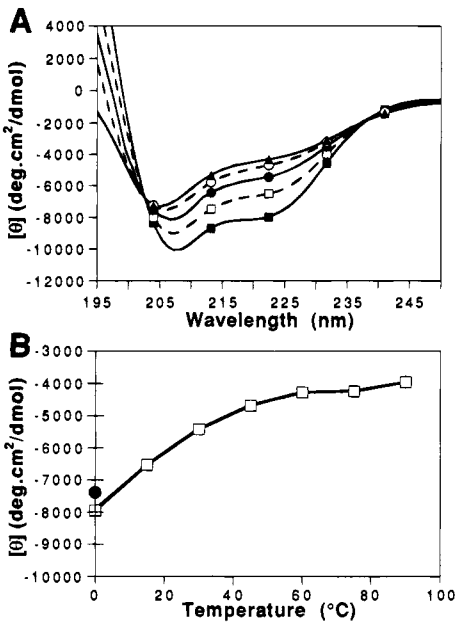

Figure 3. Thermal melting of peptide **3**: (A) CD spectra of 50 μM peptide **3** in 10 mM sodium phosphate buffer, pH 7.0, measured at increasing temperatures of 0 °C (■), 15 °C (□), 30 °C (●), 45 °C (○), and 60 °C (▲); (B) mean residue ellipticity of peptide **3** in aqueous buffer at 222 nm, plotted as a function of increasing temperature (□), and after annealing (●).

The low α-helix content expected for peptide **2** by visual estimation of the aqueous CD spectrum was also confirmed by both analyses (Tables 1 and 2). The small ellipticities observed for this spectrum, relative to the spectra of hCT and peptides **1** and **3**, were attributed to an increase in the β-sheet component of the Brahms and Brahms standard spectra, and by increased contributions due to component 3 of the Park and Fasman basis set, which these authors attribute to the aromatic and disulfide-bridge structures.[40] However, neither type of linear combination could fit the CD spectrum of peptide **2** as well as the spectra of the other analogues, indicating that there may be an additional component to this spectrum that is not represented by either of the basis sets used in these analyses.

To examine the stability of the helix-stabilized conformation of peptide **3**, thermal denaturation studies were performed by measuring CD spectra for this peptide as a function of temperature. Starting at 0 °C, the temperature of a 100 μM peptide **3** solution in aqueous 10 mM phosphate buffer (pH 7.0) was increased to 90 °C in steps of 15 °C. The spectra obtained at each temperature formed a nested set with a crossover point at 203 nm (Figure 3A), consistent with a gradual melting of the helical structure to form disordered structure with increasing temperature.[39] At 0 °C, a significantly higher α-helical content than that observed

Table 2. Quantitative Analysis of Circular Dichroism Spectra by Linear Combination of the Protein-Derived Basis Set of Park and Fasman[40]

peptide[b]	basis set content (%)[a]				
	component 1 (α-helix)	component 2 (β-turn and/or parallel β-sheet)	component 3 (aromatic and disulfide)	component 4 (unordered and/or γ-turn)	component 5 (antiparallel β-sheet)
hCT	2 (3)	none	25	56 (75)	16 (22)
peptide 1	5 (6)	none	23	54 (71)	18 (23)
peptide **2**	3 (5)	none	36	42 (65)	19 (29)
peptide **3**	13 (17)	none	26	45 (61)	17 (22)

[a] Values in parentheses indicate the secondary structure contents (%) calculated as 100 times the basis weight of each component divided by the sum of the basis weights for the secondary structure components 1 + 2 + 4 + 5.[40] [b] Peptide spectra were measured in 10 mM sodium phosphate buffer, pH 7.0, at 25 °C.

at 25 °C was indicated by the stronger negative ellipticities at 208 and 222 nm, and at 60–90 °C, the signal had reached a plateau with a lower but significant amount of ordered secondary structure remaining. This interpretation of the conformational melting in terms of a helix-coil transition was supported by quantitative analyses of the spectra by least-squares fit to the standard spectra of Brahms and Brahms[39] or Park and Fasman[40] (data not shown). A plot of $[\theta]_{222}$ *versus* temperature (Figure 3B) indicates that the melting transition was broad and noncooperative, as is typical for monomeric peptides that are partially folded at room temperature. The CD spectrum and $[\theta]_{222}$ value obtained when the peptide solution was cooled back down from 90 °C to 0 °C were nearly indistinguishable from those obtained initially. To ensure that the above results were not influenced by possible peptide degradation during the thermal denaturation procedure, analytical HPLC of the initial peptide solution and of that recovered after that procedure, including co-injection of both solutions, was performed. No changes in the analytical HPLC profiles were observed, confirming the chemical stability of peptide **3** during the melting experiment.

In order to investigate the helix-forming propensity of the lactam-bridged hCT analogues further, CD spectra were also measured in 50% aqueous TFE, a solvent mixture that is generally observed[42] to have a helix stabilizing effect. All four peptides showed increased α-helix contents in this solvent system, in the order hCT = peptide **1** > peptide **3** > peptide **2**, as judged by the shapes of the CD curves and the negative ellipticities at 222 nm (Figure 2B). The CD spectra determined for hCT and peptide **1** in 50% TFE were essentially superimposable and similar to that reported previously for hCT in 40% TFE.[43] NMR studies indicate that the major conformer of hCT in this mixed solvent system includes a distorted α-helical structure formed by residues 9–22.[41] Our results suggest, therefore, that peptide **1** also adopts a helical conformation in its central portion in this mixed solvent. Again, peptide **2** was noteworthy for having a very low secondary structure content, even in these helix promoting conditions. Surprisingly, peptide **3** showed only a moderate increase in the $-[\theta]_{208}$ and $-[\theta]_{222}$ signals in 50% aqueous TFE ($[\theta]_{222} = -8520$ deg·cm²/dmol) compared to its aqueous solution conformation ($[\theta]_{222} = -5880$ deg·cm²/dmol), indicating that the effects of TFE on the secondary structure of this peptide are complex.

Rat Brain Receptor Binding Assays. The salmon calcitonin radioligand [^{125}I-Tyr^{22}]sCT binds to specific sites in rat brain membrane preparations that presently have an unknown functional role. Unlabeled sCT, but not hCT (which is structurally much closer to rat calcitonin[15]), competes effectively with [^{125}I-Tyr^{22}]sCT for binding to these sites in a kinetic fashion, but cannot be used effectively to wash out the radioligand after it bound.[44,45] However, the rat brain [^{125}I-Tyr^{22}]sCT radioreceptor binding assay is often a good predictor for the *in vivo* biological activity of the calcitonins.[44–46] Therefore, in order to begin to evaluate the biological activity of the three lactam-bridged hCT analogues, competitive inhibition of the specific rat brain receptor binding of [^{125}I-Tyr^{22}]sCT by sCT (the strongest known naturally occurring inhibitor[44]), hCT (a weak inhibitor[44]), and the three hCT analogues was compared. As shown in Figure 4, peptide **2** (IC_{50} = 63 nM) is 80-fold more potent than hCT (IC_{50} = 5000 nM) as an inhibitor of radioligand binding, although it is still 80-fold less potent than sCT (IC_{50} = 0.8 nM). In contrast, only small increases in inhibitory potency are exhibited by the two other analogues, peptides **1** and **3**, compared to hCT. The significant difference in potency observed for peptides **1** and **2** in this assay indicates that inhibition of radioligand binding is very sensitive to the exact nature of the lactam-bridge structure linking positions 17 and 21. The low potency of peptide **3** in this assay indicates that there is also no direct correlation of inhibitory potency with α-helix content in aqueous solution.

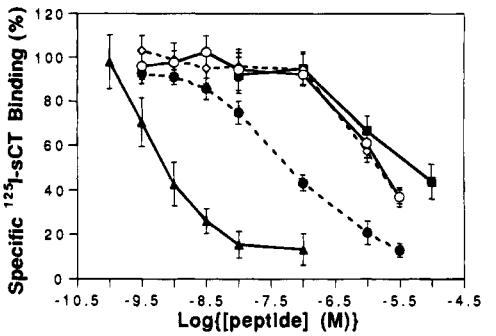

Figure 4. Binding of peptides to ^{125}I-sCT-labeled sites in rat brain membranes at 4 °C. Specific radioligand binding is plotted as a function of the concentration of competing sCT (▲), hCT (■), peptide 1 (◇), peptide **2** (●), and peptide **3** (○). Each point of the binding isotherms represents the mean ± SEM for three or four independent experiments in which each competing ligand concentration had been assayed in triplicate.

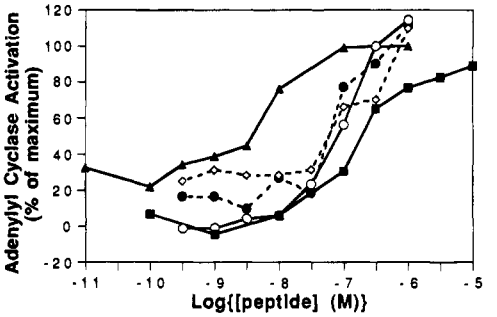

Figure 5. Peptide activation of adenylyl cyclase in kidney membranes. Adenylyl cyclase activity above basal levels is plotted as a function of peptide concentration for sCT (▲), hCT (■), peptide 1 (◇), peptide **2** (●), and peptide **3** (○). Each point is the mean of two to four separate adenylyl cyclase activation assays, in which the cAMP produced under each set of conditions was determined in duplicate by the RIA (see text).

Adenylyl Cyclase Activation Assays. To investigate the hormonal properties of the three synthetic hCT analogues further, we tested their abilities to stimulate adenylyl cyclase activity[47] in rat kidney membranes. The activities of sCT and hCT, already described in the literature,[48] were also tested in this assay system in order to ensure the validity of the assay and to compare the potencies of the lactam-bridged analogues to those of hCT (weak potency) and sCT (high potency) directly. As shown in Figure 5, all three analogues exhibited similar concentration-dependent adenylyl cyclase activation profiles, at somewhat lower concentrations than hCT. The IC_{50} values of the three analogues were all in the range 40–80 nM, which is about 3–4 times lower than the IC_{50} found for hCT (about 200 nM), but still

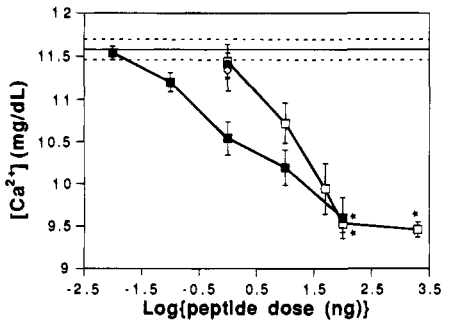

Figure 6. Hypocalcemic assay of peptides in mice. Serum calcium levels measured in groups of 5–9 mice/dose (except: *3 mice/dose) 1 h after subcutaneous injection of hCT (□), peptide 1 (●), peptide 2 (■), or peptide 3 (◇) are plotted as a function of the peptide dose. Data points indicate the mean value for the group ± SEM. The basal [Ca^{2+}] value ± SEM (21 mice) is indicated by the solid and broken lines. Peptides 1 and **3** were tested at only one dose, as indicated.

at least 10 times higher than that of sCT (4 nM). Full agonist activity was also demonstrated for peptides **1**, **2**, and **3**, since the maximal stimulation of adenylyl cyclase observed at the higher concentrations studied was comparable to that of sCT or hCT. These results clearly indicate that each of the conformational constraints imposed on hCT in the three analogues not only meet the requirements for rat kidney receptor binding and signal transduction but also contain structural or conformational features that improve the net agonist potency of the human hormone.

***In Vivo* Hypocalcemic Assay.** The hypocalcemic effect of the calcitonins *in vivo* is a complex function of their bioavailability and pharmacological potency combined but is generally the most direct measure of their therapeutic potential.[13,15,49] We therefore performed *in vivo* hypocalcemic assays on the three analgoues and hCT using various peptide doses injected sc at the dorsal neck in mice and then analyzing blood samples for serum calcium 1 h after injection.[29] Initially, each peptide was tested at a dose of 1 ng, and hypocalcemic effects were compared with those of various doses of hCT (Table 2). A 1 ng dose of peptide **2** produced a marked and statistically significant reduction in serum Ca^{2+} (10.54 *versus* 11.58 mg/dL in mice injected with the control saline solution only), corresponding to 49% of the maximal observed reduction (ΔCa^{2+}_{max}) produced by hCT (2000 ng dose). By comparison, 1 ng of hCT only caused a reduction corresponding to 7% of the maximum effect. Peptides **1** and **3** also only showed weak activity when administered at the 1 ng dose (8% ΔCa^{2+}_{max} and 11% ΔCa^{2+}_{max}), which indicates a correlation of the *in vivo* hypocalcemic effects with the rat brain receptor binding potencies, but not the adenylyl cyclase activation potencies. Since peptide **2** was found to cause a strong and statistically significant reduction of serum Ca^{2+} levels in these initial studies, we then tested whether the hypocalcemic effect of **2** was dose-dependent. Activities of peptide **2** were tested over a wide dose range (0.01–100 ng), and serum Ca^{2+} levels were again compared to those obtained from control mice (Figure 6). A sigmoidal dose–response curve was observed that indicated 10–20-fold higher hypocalcemic potency than hCT at the EC_{50} dose levels and the 1 h time point after sc injection. The maximal hypocalcemic effects observed for both peptide **2** and hCT were also similar.

Discussion

The role of amphiphilic α-helical structures in biologically active peptides in determining their functions, though widely investigated, still remains to be elucidated.[3,4] Structure–activity studies of several peptide hormones, including β-endorphin, glucagon, CRF, parathyroid hormone-related protein, and salmon calcitonin, have generally been indicative of the strong correlation between amphiphilic α-helical structure and pharmacological activity.[3,4] In the case of calcitonin, secondary structure predictions as well as a number of structure–activity relationship studies of calcitonins have correlated the potential amphiphilic α-helical domain between residues 8 or 9 and 21 or 22 with pharmacological potency.[15–23] For example, high helix contents in solution or bound to amphiphiles such as SDS or dimyristoylphosphatidylcholine correlate well with receptor-binding and hypocalcemic potencies,[17] and minimally homologous sCT analogues that retain the physicochemical properties characteristic of the amphiphilic α-helix also retain high potency in pharmacological assays.[21–23] Furthermore, deletion of residue 16 from sCT or hCT, which is near the center of the proposed helical structure in residues 8 or 9 through 21 or 22, results in substantial loss of pharmacological potency.[26] However, analogues based on [des-Leu^{19}]sCT that have lost the phospholipid-binding properties associated with the sCT amphiphilic α-helical structure nevertheless retain most of the *in vivo* hypocalcemic potency of native sCT.[25] In addition, the high hypocalcemic activity reported[24] for [Gly^{8}]sCT does not fit with simple expectations for a required α-helix at the N-terminal end of the proposed amphiphilic structure, and analogues of sCT with multiple deletions in residue positions 19–22 also retain high potencies *in vivo*, indicating that the C-terminal end of the proposed helix is not essential either.[30]

In order to understand the relationship between the amphiphilic α-helical region in human calcitonin (hCT) and its bioactivities, we have synthesized analogues of hCT that have lactam bridges with known helix-stabilizing properties[5–7,10,12] incorporated into the N-terminal or the C-terminal segments of this proposed structure (Figure 1). Solid-phase methodology was used, either with direct side chain to side chain cyclization on the solid support[5] or in combination with the separate synthesis of protected cyclic segments using the oxime resin method.[33,34] While both synthetic methods gave products in similar, satisfactory yields (between 10 and 25% after purification), the former method had the additional advantage of being simpler and more rapid.

CD studies of the synthetic peptides and hCT, in aqueous buffer, at pH 7.0 (Figures 2 and 3, Tables 1 and 2) showed a modest increase in α-helical structure relative to hCT only for peptide **3**, which contained a Lys^{i}, Asp^{i+4} lactam bridge near the N-terminal region of the potential amphiphilic α-helical domain of hCT. Little or no additional helical structure was observed upon introduction of either a Lys^{i}, Asp^{i+4} or an Asp^{i}, Lys^{i+4} lactam bridge into the C-terminal part of the proposed amphiphilic α-helix. This finding of a strong sequence-context dependency for the helix-inducing effect of these conformational constraints contrasts significantly with the earlier studies cited of amphiphilic

α-helical peptide hormones and model peptides.[5-7,10,12] It is clear from this result and the earlier studies that the helix-stabilizing effect of such constraints is modest and may only be worth about 1 kcal/mol. Thus, the nature of the specific residues in the native sequence that have been substituted to form the bridge, and also the amino-acid sequences on either side of the bridged positions, which must be able to propagate the helical structure along the peptide chain, are expected to have a significant influence on the increase in helix content observed. In this case, the greatest increase in helix content was obtained when one of the residues substituted in forming the bridge was a glycine residue, which is known for its helix destabilizing properties.[31,50] Even for peptide **3**, however, the increase in helix content was small, reflecting the underlying instability of the α-helical conformation in hCT in aqueous solution.

Perhaps the most surprising result from our CD studies comes from the comparison of peptides **1** and **2**, which have lactam bridges that have both previously been characterized as helix stabilizing[5,6] placed in the same positions in the peptide chain (residues 17 and 21), but oriented in opposite directions. This study shows that these Lys^{i}, Asp^{i+4} and Asp^{i}, Lys^{i+4} bridges are not necessarily equivalent in their conformational effects and may give different results in the same sequence context. In this case, the reduced intensity of the minimum at around 200 nm in the CD spectrum of peptide **2** and the lack of a significant helix signal at 222 nm (Figure 2) indicate that the Asp^{17}, Lys^{21} bridge in this analogue gives rise to a more ordered, but unidentified, nonhelical conformation (Tables 1 and 2), either in aqueous solution or in 50% TFE. In contrast, the Lys^{17}, Asp^{21} bridge in peptide **1** appears to have only a modest conformational effect when compared to hCT in either solvent. The nonhelical character of peptide **2** is not inconsisent with the helix stabilization noted previously for Asp^{17}, Lys^{21} lactam bridges in other contexts.[5,6] Rather, it indicates that alternative, ordered conformations have been stabilized over the predominantly disordered conformations of hCT to a greater extent than has the α-helical conformation.

In correlation with its distinctive CD spectrum, peptide **2** exhibited an 80-fold higher potency than hCT in the [^{125}I]sCT radioreceptor binding assay in rat brain (Figure 4) and a 10−20-fold increase in potency in the *in vivo* hypocalcemic assay in mice, 1 h after sc injection (Figure 6 and Table 3). In contrast, the two other lactam-bridged analogues, with similar or moderately increased helix contents relative to hCT, showed no significant increase in potency in either of these assays. This correlation suggests that there is a nonhelical structural feature, located around the bridged residues in peptide **2** at the end of the putative amphiphilic α-helix, that may determine, in part, the pharmacological actions of hCT in both the CNS of the rat and the peripheral sites of hypocalcemic action in mice (osteoclasts and, to a lesser extent, kidney).

Potencies in the rat brain radioreceptor binding assay and in hypocalcemic assays usually show a good correlation,[44-46] although the physiological function of the [^{125}I-Tyr^{22}]sCT-labeled sites in rat brain is not yet characterized. However, the potency increases observed in these assays for peptide **2** do not necessarily refect an increase in receptor affinity, in either case. SCT is a very potent competitor for [^{125}I-Tyr^{22}]sCT receptor binding in rat brain membranes, when the radioligand and competitor are added at the same time, but receptor-bound [^{125}I-Tyr^{22}]sCT is slowly and only partially displaced by the later addition of unlabeled sCT in a fashion inconsistent with an equilibrium process.[44,45] Also, quantitative differences in the hypocalcemic activities of calcitonins of various species, and the duration of the hypocalcemic response, have been shown to be inconsistent with the peptide ligand metabolic clearance rates.[15,51] In these assays, receptor binding rates may be a significant factor, and the response that is measured may be under significant kinetic control. In this case, the potencies of peptide ligands binding by a "zipper" type of mechanism[52] should correlate well with the population in aqueous solution of the conformation required for the initial receptor recognition step, rather than the conformation adopted in the final ligand−receptor complex.

Table 3. *In Vivo* Hypocalcemic Effects of Peptides in Mice 1 h after Subcutaneous Injection

peptide	dose (ng)	serum [Ca^{2+}] (mg/dL)	ΔCa^{2+} (% of max)[b]
	0	11.58 ± 0.12	0.0
hCT	1	11.44 ± 0.20	6.6
hCT	10	10.72 ± 0.24	40.6
hCT	50	9.94 ± 0.30	77.4
peptide 1	1	11.40 ± 0.14	8.5
peptide **2**	0.01	11.54 ± 0.08	1.9
peptide **2**	0.1	11.20 ± 0.11	17.9
peptide **2**	1	10.54 ± 0.20	49.1
peptide **2**	10	10.19 ± 0.21	65.6
peptide **3**	1	11.34 ± 0.24	11.3

[a] Boneferroni p values[63] were determined for the 1 ng doses of peptide analogues and were found to be significant for peptide **2** *versus* control ($p < 0.001$), peptide **2** *versus* hCT (1 ng, $p < 0.05$), peptide **2** *versus* peptide 1 ($p < 0.05$), but were not significant for hCT (1 ng) *versus* control, peptide **2** *versus* hCT (50 ng), and peptide **2** *versus* peptide **3**. [b] Hypocalcemic activities are expressed as percent of the hypocalcemic effect of a 2000 ng dose of hCT, which had been determined to cause a maximal reduction in serum Ca^{2+} levels (Figure 6).

^{1}H-NMR studies of hCT in a mixed solvent system, chosen to mimic the reduced water activity expected at the membrane/receptor surface, indicate a type I β-turn centered around residues 18 and 19 connecting two short strands of β-sheet.[53] Furthermore, the NMR-derived conformation is described as placing the amino-acid side chains in positions 17 and 21 on the same side of the β-sheet/β-turn structure. A similar chain reversal could be stabilized by the Asp^{17}, Lys^{21} lactam bridge in peptide **2**. The potential importance of residue 17 in stabilizing a β-turn centered around residues 18 and 19 is also supported by amino acid sequence considerations. The diverse amino acid sequences of the native calcitonins all have either Asn or His in position 17,[15] each of which has a high probability of being found in the first position of the four residues in a β-turn.[31] These residues both have side chains that can stabilize the β-turn conformation by hydrogen bonding to the central amide bond in the turn. Indeed, Asn is well-recognized as a β-sheet terminator that specifically favors initiation of a type I β-turn (i.e., the same structure found by ^{1}H-NMR) through hydrogen bonding of its side-chain carbonyl with the backbone N^{α}-H of the $i + 2$ residue.[50] In peptide **2**, our molecular modeling indicates that such a side-chain interaction is still possible, and the Asp^{17}, Lys^{21} lactam bridge might stabilize this turn further by fixing the Asp^{17} side-chain carbonyl in a position favor-

able for this hydrogen bonding. In contrast, peptide **1**, which is less potent in the brain receptor binding and hypocalcemic assays, has the bridging amide in quite a different position, remote from the proposed β-turn, and no longer has the same hydrogen bonding capability. Conformations such as this, which would bring the N-terminal and C-terminal portions of calcitonin into closer proximity, have long been proposed for the active conformation of calcitonin.[54] More recently, they have also been suggested to explain the negative correlation of hypocalcemic potency with helix content and phospholipid binding by [Gly^8]-des-Leu^{19} sCT analogues.[25]

In the rat kidney adenylyl cyclase activation assay, all three synthetic analogues showed similar potencies, each about 5-fold higher than that of hCT (Figure 5). The maximal stimulatory effects observed for these three peptides were also all in the same range as those for sCT and hCT, indicating full agonist for the analogues. These results suggest full compatibility of all of the conformationally restricted peptides with the requirements for rat kidney receptor binding and signal transduction. Taking all of the pharmacological activities of three peptides together, a functional role in calcitonin receptor recognition for the proposed amphiphilic α-helix in residues 8–21, possibly as the final conformational state adopted by the peptide ligand on the receptor, is strongly indicated. Amino acid substitutions[27,28] or deletions[23,25,26] at hydrophobic positions in this region of hCT are clearly demonstrated to have a significant effect on potencies in these assays. Therefore, one or more of the three bridges studied, which span some of these sensitive hydrophobic positions but on the opposite, hydrophilic face of an α-helix, would reasonably be expected to block receptor binding and/or activation, if the calcitonin–receptor complex(es) ultimately included a nonhelical conformation in calcitonin residues 8–21.

The different structure–activity relationship observed in the kidney adenylyl cyclase assay, compared to the rat brain receptor binding and hypocalcemic assays, is not without precedent and might reflect calcitonin receptor heterogeneity, as suggested previously.[55,56] Indeed, it has been proposed that adenylyl cyclase activation in the rat kidney has a requirement for the central α-helical structure whereas the same activity in rat brain does not,[56] and our results are consistent with this interpretation. N-Terminal deletion analogues studied previously[20] also indicate that the requirements for adenylyl cyclase activation can be differentiated from those of hypocalcemic activity by deletion of residues 1–7.

At present, the direct evidence from receptor cloning and expression for different calcitonin receptor types in the rat CNS and kidney that might be responsible for the observed variations in structure–activity relationships is inconclusive. Two isoforms of the calcitonin receptor in rat brain, C1a and C1b, have recently been cloned and expressed in a functional form in COS cells.[57,58] However, [^{125}I]sCT has an apparent affinity about 10-fold higher for the reconstituted C1a isoform,[57,58] indicated that this is probably the only one that is labeled in the rat brain membrane [^{125}I]sCT binding assays we (Figure 4) and others have performed. The limited structure–activity relationships reported support this conclusion.[57] Also, reverse transcription of mRNA and PCR amplification indicates, qualitatively, that the C1a isoform is the receptor isoform predominantly expressed in the peripheral tissues, including the kidney,[57,58] and no other rat calcitonin receptor genes have been reported to date.

As an alternative hypothesis, we suggest that potencies in the rat kidney adenylyl cyclase assay might reflect ligand–receptor interactions at equilibrium more closely than do potencies in the rat brain receptor-binding assay. This difference is supported by receptor binding studies using kidney membranes,[48] which indicate that specific binding of [^{125}I]sCT is rapidly reversed by addition of excess unlabeled sCT, in contrast to the situation in brain membranes. The higher potencies compared to hCT of peptides **1**, **2**, and **3** in the adenylyl cyclase assay may then arise from stabilization of the helical conformation in residues 8–21, if this is the conformation ultimately acquired by calcitonin in its receptor complex. From earlier studies,[5–7,10,12] we can expect such a receptor-bound helix to be stabilized by each of the three lactam bridges in the hCT analogues, even though the helix content of these peptides in solution is only increased significantly for peptide **3**, and another, nonhelical conformation is more strongly favored in solution by peptide **2**.

Conclusions

We have demonstrated that the conformational and pharmacological effects of introducing Lys^i, Asp^{i+4} and Asp^i, Lys^{i+4} side-chain lactam bridges into the potential amphiphilic α-helical domain in hCT residues 8–21 or 8–22 depend strongly on the location and nature of the bridges. The results indicate full compatibility of the peptide design, which was based on stabilization of this α-helical structure, with the pharmacological activities tested. However, correlations with the solution conformations of the analogues indicate the potential importance of another, nonhelical conformation in determining potency in rat brain receptor binding and hypocalcemic activity in mice. These results are compatible with the β-sheet/β-turn structure identified by Motta *et al.* in the solution conformation of hCT residues 17–21 in DMSO/H_2O (85/15, v/v).[53] Overall, our results also support the suggestion of these authors that the calcitonin function may involve this β-turn structure or a similar chain reversal in an initial receptor recognition step, followed by a conformational change to α-helix in the amphiphilic α-helical region, when the final receptor-bound conformation is attained. This process is similar, as Motta *et al.* suggest,[53] to the model proposed by Gierasch and colleagues for signal- or leader-peptide function in determining protein translocation across the periplasmic membrane in bacteria[59] and would seem to be an appropriate process by which a multiconformational ligand such as hCT in solution might initiate interactions with a membrane or receptor surface and, subsequently, still be able to realize the surface-binding potential of the amphiphilic structure contained within its sequence.

Our finding that an Asp^{17}, Lys^{21} lactam bridge both stabilizes an ordered, nonhelical conformation in hCT that may include the β-turn structure discussed above, and also improves its hypocalcemic potency *in vivo* by at least at least an order of magnitude, may have important therapeutic applications. First, it will be

interesting to see whether the other more potent calcitonin structures that are currently in therapeutic use, such as sCT or the eel calcitonin analogue, aminosuberic[1,7] eel calcitonin (elcatonin[32]), can also attain higher potencies with the same Asp[17], Lys[21] lactam-bridge modification. Second, the time course of the hypocalcemic effect of peptide **2** and these additional lactam-bridged analogues, if they are more potent, should be investigated. It is reasonable to expect that their conformational restrictions will reduce their rates of proteolysis *in vivo*, and this may enhance the duration of the hypocalcemic effects beyond those of the parent compounds. Indeed, lactam-bridged GRF analogues with longer plasma half-lives have been shown to have *in vivo* effects that are also of longer duration.[5,60] Finally, it is important to determine more precisely the nature of the aqueous solution conformation of peptide **2**, in order to investigate the β-turn and conformational switching hypotheses for the active conformations of hCT. This information should aid in the design of new peptidomimetics for the central region of the calcitonins. In particular, more potent hCT analogues with minimal structural changes have potential for therapeutic use in patients with immune responses to sCT or elcatonin. To date, the most potent hCT analogues reported[27,28] are, to our knowledge, [Leu[12,16,19],Tyr[22]]hCT, [Leu[0,8,12]]-hCT, and [Leu[0,8,12,16]]hCT, each of which has a greater degree of amino acid substitution and greater homology to sCT and elcatonin than does peptide **2**.

Experimental Section

Materials and Methods. Protected L-amino acids were purchased from Bachem Bioscience Inc. and Advanced ChemTech. *p*-Methylbenzhydrylamine resin (MBHA) (0.65 mmol/g) for solid-phase syntheses was purchased from Advanced ChemTech. MeOH, EtOH, EtOAc, and ethyl ether were of ACS grade (Fischer Scientific) and were used without further purification. DCM (Fischer Scientific; ACS grade), DMF, and iPrOH (Aldrich; HPLC grade) were stored over 4 Å molecular sieves (Aldrich). DIEA (Aldrich) was distilled over ninhydrin and also stored over 4 Å molecular sieves. TFA was purchased from Halocarbon and was used without further purification. BOP and HBTU were purchased from Novabiochem, HOBt was purchased from Advanced ChemTech, and DCC was purchased from Fluka. Pyridine, piperidine, acetic anhydride, TFE, theophylline, $MgCl_2$ (ACS grade), NaF (ACS grade), and bacitracin were purchased from Aldrich. Synthetic human and salmon calcitonins for CD studies, receptor binding, and adenylyl cyclase assays were purchased from Bachem California. Reagents for the adenylyl cyclase assay, including creatine phosphokinase (190 units/mg of solid), adenosine 5′-triphosphate disodium salt (grade I: from yeast), phosphocreatine disodium salt hydrate, TCA, and BSA (prepared from Fraction V; essentially fatty acid free) were purchased from Sigma. Salmon [^{125}I-Tyr[22]]calcitonin (specific activity 2000 Ci/mmol) was purchased from Amersham.

For amino acid analysis, peptides were hydrolyzed in 6 N HCl (Pierce) at 110 °C for 24 h, and peptide resins in 12 N HCl/propionic acid (1/1) (Pierce) at 130 °C for 18 h. Phenol was added for peptides containing tyrosine residues. Ion-spray mass spectrometry (Dr. Hanno T. Langen, Hoffmann-La Roche, Basel, Switzerland) was used to determine the mass of the end products. Reverse-phase HPLC was performed on a Rainin HPLC system (consisting of two HPLX pumps connected to a Rainin electronic pressure module, a Dynamax Model UV-D multiwavelength detector, a Rheodyne Model 7125 manual injection valve, and a Macintosh compatible PC for gradient control and data analysis), or on a Perkin-Elmer HPLC system (consisting of a Perkin-Elmer series 410B10 LC pump, a Perkin-Elmer LC 90 UV detector and a Hewlett-Packard HP 3390A integrator). Peptides were eluted on C_{18} Dynamax-300A columns with a 5 μm particle size (4.6 mm × 25 cm for analytical separations, and 10 mm × 25 cm for preparative separations). Flow rates were 1.5 and 2.5 mL/min for the analytical and preparative separations, respectively. Eluting buffers were as follows: A, 0.058 % (v/v) TFA in water; B, 0.05% (v/v) TFA in 90% (v/v) CH_3CN/water. Peptides were detected at 220 nm.

Peptide Synthesis. *Cyclo*[17,21]-[Lys[17],Asp[21]]hCT (Peptide 1) and *Cyclo*[10,14]-[Lys[10],Asp[14]]hCT (peptide 3). Fully protected peptidyl-resins N^{α}-Boc-(hCT(22−32))MBHA (**4**) and N^{α}-Boc-(hCT(15−32))MBHA (**5**) were synthesized according to standard solid-phase synthesis procedures. Throughout the syntheses N^{α}-Boc-L-amino acid derivatives were used. For trifunctional amino acids, the following side-chain protection was used: Asp(β-OcHx), Cys(S-*p*-MeBzl), Glu(γ-OBzl), His(π-Bom), Lys(2Cl-Z), Thr(Bzl), and Tyr(2Br-Z). To attach the C-terminal Pro residue to the resin, previously neutralized MBHA resin (4 g, 0.65 mmol/g) was reacted with Boc-Pro-OH (1.68 g, 7.2 mmol) and DCC (1.6 g, 7.2 mmol) in DCM (30 mL) for 18 h (substitution level 0.62 mmol/g resin according to picric acid analysis). The resin was subsequently acetylated with Ac_2O (2.5 mL, 26 mmol) in the presence of pyridine (2.1 mL, 26 mmol) for 1 h. Peptide chain elongations were then performed by applying the DCC/HOBt coupling method (3-fold excess) in DMF in or mixtures of DMF/DCM (4/1, v/v). Couplings were performed once except for Ile[27], Phe[22], and His[20], which were coupled twice. Coupling completeness was followed using the Kaiser ninhydrin test. For cleavage of the Boc group, 50% TFA in DCM was used (30 min), with the exception for Gln[24] for which 4 N HCl in dioxane (30 min) was used. Substitution levels were estimated to be 0.57 mmo/g for the N^{α}-Boc-(hCT(22−32)MBHA resin (**4**) and 0.52 mmol/g resin for N^{α}-Boc-(hCT(15−32)MBHA resin (**5**), based on picric acid analysis; amino acid analysis of **4** gave Ala (2) 2.00, Gln (1) 1.04, Gly (2) 2.10, Ile (1) 1.05, Phe (1) 1.08, Thr (1) 0.84, Val (1) 1.10; amino acid analysis of **5** gave Ala (2) 2.00, Asx (2) 1.91, Gln (1) 0.95, Gly (2) 2.15, His (1) 0.90, Ile (1) 1.08, Lys (1) 0.96, Phe (3) 2.89, Thr (2) 1.82.

Side-chain protected N^{α}-Fmoc-*cyclo*[17,21]-[Lys[17],Asp[21]]hCT-(17−21)-OH (**6**) and N^{α}-Fmoc-*cyclo*[10,14]-[Lys[10],Asp[14]]hCT(10−14)-OH (**7**) were synthesized by head-to-tail cyclization using the Kaiser oxime resin and a four-dimensional orthogonal protection scheme (Boc/Bzl/Fmoc/Al), as we described recently.[34] For the synthesis of peptide 1, resin **4** (516 mg, 0.17 mmol) was treated with 50% TFA in DCM, neutralized with 5% DIEA, and then washed and swollen in DMF. Thereafter, a DMF solution (2.5 mL) of cyclic fragment **6** (128 mg, 0.11 mmol), HBTU (83 mg, 0.22 mmol), and HOBt (30 mg, 0.22 mmol) was added. DIEA (192 μL, 1.1 mmol) was added, and the reaction mixture was shaken for 24 h, followed by filtration and washing of the peptidyl-resin with DMF (3×), iPrOH (1×), and DCM (2×). The yield of this coupling was 63%, as judged by quantitative spectrophotometric determination of the dibenzofulvene−piperidine adduct moiety at 290 nm, after cleavage of the Fmoc group by 20% (v/v) piperidine in DMF. To cap unreacted amines after this segment condensation reaction, the resultant fully protected N^{α}-Fmoc-*cyclo*[17,21]-[Lys[17],Asp[21]]-hCt(17−32)-MBHA resin (**8**) (substitution level 0.23 mmol/g resin, as estimated by Fmoc cleavage) was acetylated with Ac_2O (151 μL, 1.6 mmol) in the presence of DIEA (279 μL, 1.6 mmol) in DCM (3 mL) for 45 min.

For the synthesis of peptide **3**, resin **5** (650 mg; 0.14 mmol) was N^{α}-deprotected, neutralized, and washed, as described above for **4**. Then, a DMF solution (3.5 mL) of **7** (216 mg, 0.18 mmol), HBTU (134 mg, 0.36 mmol), and HOBt (48 mg, 0.35 mmol) was added. DIEA (169 μL, 0.97 mmol) was added, and the reaction mixture was shaken for 3 h, the progress of the coupling being followed by HPLC. Thereafter, the peptidyl-resin was washed and acetylated as described above. Fully protected N^{α}-Fmoc-*cyclo*[10,14]-[Lys[10],Asp[14]](hCt(10−32))-MBHA resin (**9**) was thus obtained, having a substitution level of 0.40 mmol/g of resin (yield of the coupling 77%) as estimated by Fmoc cleavage.

To complete the syntheses of peptides 1 and **3**, peptidyl-resins **8** and **9** were treated with 20% piperidine in DMF (1 × 1 min and 1 × 20 min) and washed. Elongation of the peptide

chains toward the N-terminus was then performed by standard solid-phase synthesis methods. For peptide 1 synthesis, couplings were performed by the preformed symmetrical anhydride method, except for Boc-Gln and Boc-Asn, for which the DCC/HOBt method was used. For peptide **3**, the BOP method of coupling was used, and double couplings at Leu[9] and Thr[6] were required. Portions (100 mg) of the resultant fully protected peptidyl-resins N^{α}-Boc-*cyclo*[17,21]-[Lys[17],Asp[21]]-hCT-MBHA (**10**) and N^{α}-Boc-*cyclo*[10,14]-[Lys[10],Asp[14]]hCT-MBHA (**11**) were N^{α}-Boc deprotected and neutralized and then treated with 6 mL of a mixture of HF/anisole/DMS/*p*-thiocresol (10/1/1/2, v/v/v/w) containing 0.27 M cysteine for 30 min at −5 °C, then 1 h at 0 °C). After Et_2O precipitation and Et_2O washes (3×) of the deprotected peptides, crude peptides 1, and **3**, in reduced form, were extracted with 10% (v/v) HOAc (4 × 20 mL), lyophilized, and subjected to air oxidation in 0.1 M NH_4HCO_3 under high dilution conditions (1×10^{-4} M), in the dark, over 24 h. Upon completeness of the oxidations, which were followed by HPLC the mixtures were acidified (pH 4−5) by addition of 1 M HCl, and the solutions were then lyophilized. Crude products 1 and **3** were subsequently purified by preparative reverse-phase HPLC (conditions described under materials and methods) to give peptides 1 and **3** of high purity, as confirmed by HPLC analysis and ion-spray mass spectrometry. Amino acid analysis of 1 gave Ala (2) 2.00, Asx (3) 2.51, Gln (2) 1.91, Gly (4) 3.88, His (1) 0.91, Ile (1) 1.03, Leu (2) 1.97, Lys (2) 2.06, Met (1) 1.06, Phe (3) 3.06, Pro (2) 1.97, Ser (1) 0.83, Thr (4) 3.40, Tyr (1) 0.94, Val (1) 1.03; amino acid analysis of **3** gave Ala (2) 2.00, Asx (4) 3.48, Gln (1) 0.99, Gly (3) 2.99, His (1) 0.93, Ile (1) 1.01, Leu (2) 2.12, Lys (2) 2.15, Met (1) 1.16, Phe (3) 3.25, Pro (2) 1.97, Ser (1) 0.87, Thr (5) 4.14, Tyr (1) 0.96, Val (1) 0.99; ion-spray MS for 1 gave 3428 ± 0.8 (calcd 3428.9 for $[M + H]^+$ average mass), and for **3** gave 3458 ± 0.6 (calcd 3458.97 for $[M + H]^+$ average mass).

***Cyclo*[17,21]-[Asp[17],Lys[21]]hCT (Peptide 2).** The synthesis was performed according to the method of Felix et al.[5] Briefly, peptidyl-resin **4** (500 mg, 0.17 mmmol) was coupled with Boc-Lys(Fmoc) (47 mg, 0.1 mmol) and subsequently acetylated with Ac_2O (94.7 μL, 1 mmol) and pyridine (80.7 μL, 1 mmol). The "diluted" peptidyl-resin obtained (substitution level 0.21 mmol/g resin, estimated by Fmoc cleavage) was then elongated until residue Asp[17], which was coupled as Boc-Asp(OFm). Side-chain protecting groups used were otherwise the same as those used for the syntheses of peptides 1 and **3**. Cleavage of the Fmoc and OFm side-chain protecting groups on residues 21 and 17, respectively, proceeded by treatment with 20% piperidine in DMF, as described.[5] Side chain to side chain cyclization was performed by treatment with HBTU (114 mg/0.30 mmol) and DIEA (60 μL, 0.34 mmol) in DMF (50 mL) for 4 h and then repeated once (2 h). Thereafter, the peptidyl-resin was washed and acetylated. The incorporation of the remaining residues was then performed by using the symmetrical anhydride and DCC/HOBt methods (double couplings for Leu[4] and Asn[3]), as described for the synthesis of peptide 1. HF cleavage of portions (100 mg) of the side-chain-protected peptidyl-resin, NH_2-*cyclo*[17,21]-[Asp[17],Lys[21]]hCT-MBHA (**12**) and subsequent extraction and air oxidation were performed as described for the syntheses of 1 and **3**. Preparative reverse-phase HPLC purification gave peptide **2** of high purity, as shown by HPLC analysis and ion-spray mass spectrometry. Amino acid analysis of **2** gave Ala (2) 2.00, Asx (3) 2.41, Gln (2) 1.94, Gly (4) 3.94, His (1) 0.88, Ile (1) 0.96, Leu (2) 1.84, Lys (2) 1.94, Met (1) 0.96, Phe (3) 2.82, Pro (2) 1.84, Ser (1) 0.96, Thr (4) 2.96, Tyr (1) 0.85, Val (1) 1.04; ion-spray MS gave 3428 ± 0.6 (calcd 3428.9 for $[M + H]^+$ average mass).

Circular Dichroism Spectropolarimetry. Circular dichroism (CD) spectra were obtained at 25 °C using an Aviv Model 62DS spectropolarimeter (Aviv Associates) fitted with a Peltier temperature controller. Data represent the average of three scans in the range of 184−250 nm and were collected at 0.25 nm intervals, with a spectral band width of 1.5 nm and a 1.0 s integration time. The quartz cells (path length 1.0 or 10.0 mm) were washed with 30% HCl in EtOH, water, and then EtOH before use. The following two buffers were used: (1) 10 mM aqueous sodium phosphate (pH 7.0) and (2) 10 mM sodium phosphate (pH 7.0) diluted 1/1 (v/v) with TFE. Concentrations of peptide stock solutions in 1 mM HCl were determined by UV measurements, using $\epsilon_{274.5} = 1440\ M^{-1}\ cm^{-1}$ (the sum of $\epsilon_{274.5}$ estimated for the tyrosyl residue and the disulfide bridge) and were close to the concentrations estimated by the weight of lyophilized peptides. Ellipticities are expressed on a molar basis as mean residue ellipticity (deg·cm²/dmol).

Rat Brain Receptor Binding Assays. Crude rat brain membrane preparations and the receptor binding assays were based on a method described by Nakamuta et al.[61] Since loss of [^{125}I-Tyr[22]]sCT specific binding activity was observed using brain membranes stored at −70 °C, fresh membrane preparations were used for each assay. Male Sprague−Dawley rats (300−450 g) were decapitated, and their brains were removed and kept on ice. After discarding the cerebellum, the remaining tissue was homogenized in ice-cold 50 mM Tris-HCl buffer (pH 7.4) (30 mL), using a Tissue Tearor (Model 985−370, type 2, Biospec Products Inc.) at 30 000 rpm (1 min). The homogenate was incubated at 0 °C for 30 min and then centrifuged at 21000*g* and 4 °C for 10 min (Marathon 21K/R centrifuge, Fisher Scientific). The supernatant was discarded and the pellet washed twice with ice-cold 50 mM Tris-HCl buffer (pH 7.4) (30 mL) and once with ice-cold assay buffer (50 mM Tris-Cl containing freshly added 45 μM bacitracin, pH 7.4). Ice-cold assay buffer was then added to the membrane preparation, and the homogenate was kept at 0 °C until used for the receptor binding assay (about 1 h). Stock solutions of peptides in 1 mM HCl were diluted to the appropriate concentrations in assay buffer (in 1.5 mL polypropylene test tubes, previously pretreated with assay buffer for 2 h) immediately before the binding assay. For the binding assay, each 1.5 mL test tube (also preatreated with assay buffer) contained cold peptide in a concentration range from 1 μM (10 μM for hCT) to 100 pM, [^{125}I-Tyr[22]]sCt (9 pM), and brain membranes (approximately 1.6 mg total protein, determined by the BioRad protein assay) in a total of 1.0 mL assay buffer. Nonspecific [^{125}I-Tyr[22]]sCT binding was determined in the presence of 1 μM competing sCT. Incubation started by the addition of the chilled membrane preparation (at 4 °C), continued for 30 min at 4 °C, and was terminated by centrifugation of the tubes (Microcentrifuge Model 235B, Fisher Scientific) at 13000*g* for 10 min. Supernatants were discarded, and the tips of the assay tubes containing the pellets were cut off, placed into scintillation vials (Fisher Scintific) containing 3 mL of scintillation fluid (Ultima Gold, Packard Instrument Company), vortexted for at least 3 min each to solubilize the pellets, and then counted using a Beckman LS7000 liquid scintillation counter. Specific binding was determined as the difference between total binding and nonspecific binding and was in the range of 70−80% of the total. Since specific binding of [^{125}I-Tyr[22]]sCT to rat brain membranes is essentially irreversible[44,45] and a true equilibration of competing ligands and receptors has not been demonstrated, equilibrium constants were not determined.

Adenylyl Cyclase Activation Assay. Kidney membranes were prepared as described by Schwartz et al.[29] Briefly, male Sprague−Dawley rats (350−400 g) were sacrificed and the kidneys were removed, placed onto ice, stripped free of surrounding fat, and cut into small pieces. Then, the kidney pieces were homogenized in an ice-cold buffer consisting of 0.25 M sucrose, 0.01 M Tris-HCl, and 0.001 M Na_2EDTA (pH 7.5) using a loosely fitting Dounce Tissue Grinder (Wheaton Peastle, 7 mL, Fisher Scientific). The crude homogenate was centrifuged at 2400*g* (30 s) at 4 °C, the pellet discarded, and the supernatant centrifuged at 4000*g* (10 min) at 4 °C. To the pellet, 14 mL of chilled storage buffer consisting of 0.01 M Tris-HCl, 0.001 M Na_2EDTA, and 10 mg/mL BSA (pH 7.5) was added, and the suspension was mixed and centrifuged (10 min at 4000*g* and 4 °C). The supernatant was discarded and the wash procedure repeated twice using 10 mL storage buffer. Finally, chilled storage buffer (10 mL) was added to the membrane pellet, and the suspension was filtered through glass wool, aliquoted in test tubes, and stored at −70 °C at a protein concentration of 7.7 mg of protein/mL (determined using the BioRad protein assay). This kidney membrane preparation was found to be stable for the adenylate cyclase assay for at least 3 months. The assay was modification of

that described by Salomon et al.[62] For each assay, a test tube containing the frozen membrane suspension was slowly thawed on ice (1 h) and diluted immediately prior to the assay to a final concentration of 1.25 mg of protein/mL of 25 mM Tris-HCl (pH 7.5) (incubation buffer). Stock peptide solutions in 1 mM HCl were diluted immediately before the assay to the appropriate concentrations in incubation buffer (in siliconized polypropylene test tubes). Each assay test tube (1.5 mL, polypropylene) containing 5 mM $MgCl_2$, 20 mM creatine phosphate, 100 units mL of creatine phosphokinase, 1 mM ATP, BSA 0.065%, 65 μM Na_2EDTA, 1 mM theophylline, peptide at the appropriate concentration (ranging from 1 μM [10 μM for hCT] to 100 pM [10 pM for sCT]), and 50 μg of membrane protein in a total volume of 100 μL of incubation buffer. Test tubes containing no peptide (basal adenylyl cyclase activity), NaF (20 mM) (control for adenylyl cyclase stimulation), or 1 μM sCT (for maximal sCT-stimulated adenylyl cyclase activity) were each also included in all assays. Incubations, initiated by the addition of membranes at 4 °C, were performed at 30 °C for 15 min and stopped by the addition of 100 μL of 20% (v/v) TCA in 50 mM phosphate buffer at 4 °C. After centrifugation (Microcentrifuge Model 235, Fisher Scientific) for 10 min at 13000*g*, supernatants were transferred into 1.5 mL test tubes (on ice) and extracted three times with Et_2O (1 mL each time) that had been saturated with water. Thereafter, the tubes were rapidly frozen and lyophilized. cAMP was then quantitated by RIA, using a "cAMP[^{125}I] assay system" (Amersham) according to the manufacturer's directions. Dissociation of the antibody-bound [^{125}I]-cAMP was performed by boiling the antibody-bound fraction in 1% SDS in the RIA buffer for 7 min, followed by centrifugation (13000*g*; 5 min) and separation and counting of the supernatants in a Beckman LS7000 liquid scintillation counter (as described above). Results (Figure 5) are expressed as percent of the maximal adenylyl cyclase stimulation above the basal level, with the maximum defined as the stimulation above basal caused by 1 μM sCT.

***In Vivo* Hypocalcemic Assay**. The method used was based on previous reports of hypocalcemic effects of calcitonins in mice after sc injection.[64] Female BALB/c mice at 8–10 weeks of age (19–21 g) were injected sc in the dorsal neck with a 250 μL solution of various peptide concentrations in 0.9% (w/v) saline containing 0.1% (w/v) BSA. Control mice were injected with an equal volume of the BSA/saline solution without peptide. One hour after injection, mice were sacrificed by CO_2 inhalation, and blood was immediately collected by cardiac puncture. Blood was allowed to stand for 10 min and centrifuged at 16000 g and 4 °C (10 min), and the serum was collected. Quantitation of serum Ca^{2+} levels was performed using a colorimetric method ($OD_{575\ nm}$) with a CALCIUM kit from Sigma. Hypocalcemic activities of various peptide doses were derived from the measured Ca^{2+} levels expressed as the mean $[Ca^{2+}] \pm$ SEM (mg/dL) and were obtained from five to nine mice per dose in at least two independently performed experiments (except as noted in Figure 6). In this assay, the basal $[Ca^{2+}]$ observed in the saline controls (21 mice) was 11.58 $\pm$ 0.12 mg/dL, and a maximum hypocalcemic effect of $\Delta[Ca^{2+}] = -2.12$ mg/dL ($[Ca^{2+}] = 9.46 \pm 0.09$) was observed for 2000 ng doses of hCT. Initial studies with 0.01–1.0 ng of sCT indicated similar maximal effects. Statistical analysis was performed by comparison among mean serum Ca^{2+} levels by using ANOVA for the analysis of variants. All reported significant levels are two-sided. The De Bonferroni method[63] was used to adjust probability values for multiple comparisons.

Acknowledgment. We wish to thank the Rockefeller University protein sequencing facility for amino acid analyses and Dr. H. T. Langen and Hoffmann-La Roche (Basel, Switzerland) for the ion-spray mass spectrometric analyses. We thank Dr. N. Greenfield for valuable discussions and assistance with the CD spectroscopy. We thank Dr. J. Al Abed and Prof. Dr. W. Voelter for their help. We are grateful to Dr. J. Bernhagen for invaluable discussions and help with the hypocalcemic assay and Dr. T. Calandra for the statistical analyses. This work was supported by USPHS Grant GM38811.

References

(1) Present address: Abteilung für Physikalische Biochemie, Physiologisch-chemisches Institut, Hoppe-Seylerstr. 4, D-72076 Tübingen, Germany.
(2) Hruby, V. J. Conformational Restrictions of Biologically Active Peptides Via Amino Acid Side Chain Groups. *Life Sci.* **1982**, *31*, 189–199.
(3) Kaiser, E. T.; Kézdy, F. J. Amphiphilic Secondary Structure: Design of Peptide Hormones. *Science* **1984**, *223*, 249–255.
(4) Taylor, J. W. Amphiphilic helices in neuropeptides. In *The Amphipathic Helix*; Epand, R. M., Ed.; CRC Press: Boca Raton, 1993; pp 285–311.
(5) Felix, A. M.; Heimer, E. P.; Wang, C. T.; Lambros, T. J.; Fournier, A.; Mowles, T. F.; Maines, S.; Campbell, R. M.; Wegrzynski, B. B.; Toome, V.; Fry, D.; Madison, V. S. Synthesis, biological activity and conformational analysis of cyclic GRF analogs. *Int. J. Pept. Protein Res.* **1988**, *32*, 441–454.
(6) Fry, D. C.; Madison, V. S.; Greeley, D. N.; Felix, A. M.; Heimer, E. P.; Frohman, L.; Campbell, R. M.; Mowles, T. F.; Toome, V.; Wegrzynski, B. B. Solution Structures of cyclic Analogues of Growth Hormone Releasing Factor as Determined by Two-Dimensional NMR and CD Spectroscopies and Constrained Molecular Dynamics. *Biopolymers* **1992**, *32*, 649–666.
(7) Bouvier, M.; Taylor, J. W. Probing the Functional Conformation of Neuropeptide Y through the Design and Study of Cyclic Analogues. *J. Med. Chem.* **1992**, *35*, 1145–1155.
(8) Kirby, D. A.; Koerber, S. C.; Craig, A. G.; Feinstein, R. D.; Delmas, L.; Brown, M. R.; Rivier, J. E. Defining Structural Requirements for Neuropeptide Y Receptors Using Truncated and Conformationally Restricted Analogues. *J. Med. Chem.* **1993**, *36*, 385–393.
(9) Chorev, M.; Roubini, E.; McKee, R. L.; Gibbons, S. W.; Goldman, M. E.; Caulfield, M. P.; Rosenblatt, M. Cyclic Parathyroid Hormone Related Protein Antagonists: Lysine 13 to Aspartic Acid 17 [i to (i+4)] Side Chain to Side Chain Lactamization. *Biochemistry* **1991**, *30*, 5968–5974.
(10) Chorev, M.; Epand, R. F.; Rosenblatt, M.; Caulfield, M. P.; Epand, R. M. Circular dichroism (CD) studies of antagonists derived from parathyroid hormone-related protein. *Int. J. Pept. Protein Res.* **1993**, *42*, 342–345.
(11) Ósapay, G.; Taylor, J. W. Multicyclic Polypeptide Model Compounds. 1. Synthesis of a Tricyclic Amphiphilic α-Helical Peptide Using an Oxime Resin, Segment-Condensation Approach. *J. Am. Chem. Soc.* **1990**, *112*, 6046–6051.
(12) ÓSapay, G.; Taylor, J. W. Multicyclic Polypeptide Model Compounds. 2. Synthesis and Conformational Properties of a Highly α-Helical Uncosapeptide Constrained by Three Side-Chain to Side-Chain Lactam Bridges. *J. Am. Chem. Soc.* **1992**, *114*, 6966–6973.
(13) Symbols and abbreviations used are in accordance to the recommendations of the IUPAC–IUB Joint Commission on Biochemical Nomenclature (*Eur. J. Biochem.* **1984**, *138*, 9–37). All amino acids are of L-configuration. Additional abbreviations: BOP, (benzotriazol-1-yloxy)tris(dimethylamino)phosphonium hexafluorophosphate; Al, allyl; BSA, bovine serum albumin; DCC, *N,N'*-dicyclohexylcarbodiimide; DCM, dichloromethane; DMF, dimethylformamide, DIEA, *N,N'*-diisopropylethylamine; DMS, dimethyl sulfide; EDTA, *N,N,N',N'*-ethylenediaminetetraacetic acid; HBTU, *O*-benzotriazole-*N,N,N',N'*-tetramethyluronium hexafluorophosphate; HOBt, 1-hydroxybenzotriazole; hCt, human calcitonin; MBHA, iPrOH, 2-propanol; OFm, fluoren-9-yl methyl ester; *p*-methylbenzhydrylamine; RIA, radioimmunoassay; sCt, salmon calcitonin; TCA, tricloroacetic acid; TFA, trifluoroacetic acid; TFE, trifluoroethanol; Tris, tris(hydroxymethyl)aminoethane.
(14) Chambers, T. J.; Magnus, C. I. Calcitonin alters the behaviour of isolated osteoclasts. *J. Pathol.* **1982**, *136*, 27–36.
(15) Guttmann, S. Chemistry and structure-activity relationship of natural and synthetic calcitonins. In *Calcitonin 1980 Chemistry Physiology Pharmacology and Clinical Aspects*; Pecile, A., Ed.; Excerpta Medica: Amsterdam, 1981; pp 11–24.
(16) Merle, M.; Lefevre, G.; Milhaud, G. Predicted secondary structure of calcitonin in relation to the biological activity. *Biochem. Biophys. Res. Commun.* **1979**, *87*, 455–460.
(17) Epand, R. M.; Epand, R. F.; Orlowski, R. C. Presence of an amphiphatic helical segment and its relationship to biological potency of calcitonin analogs. *Int. J. Pept. Protein Res.* **1985**, *25*, 105–111.
(18) Moe, G. R. The structure of calcitonin determined from the design, synthesis, and study of model peptides. Ph.D. Thesis, University of Chicago, Department of Chemistry, Chicago IL, 1985; pp 11–15.
(19) Findlay, D. M.; Michelangeli, V. P.; Martin, T. J.; Orlowski, R. C.; Seyler, J. K. Conformational Requirements for Activity of Salmon Calcitonin. *Endocrinology* **1985**, *117*, 801–805.

(20) Feyen, J. H. M.; Cardinaux, F.; Gamse, R.; Bruns, C.; Azria, M.; Trechsel, U. N-terminal truncation of salmon calcitonin leads to calcitonin antagonists. *Biochem. Biophys. Res. Commun.* **1992**, *187*, 8–13.
(21) Moe, G. R.; Miller, R. J.; Kaiser, E. T. Design of a Peptide Hormone: Synthesis and Characterization of a Model Peptide with Calcitonin-like Activity. *J. Am. Chem. Soc.* **1983**, *105*, 4100–4102.
(22) Moe, G. R.; Kaiser, E. T. Design, Synthesis, and Characterization of a Model Peptide Having Potent Calcitonin-like Biological Activity: Implications for Calcitonin Structure/Activity. *Biochemistry* **1985**, *24*, 1971–1976.
(23) Green, F. R. III; Lynch, B.; Kaiser, E. T. Biological and physical properties of a model calcitonin containing a glutamate residue interrupting the hydrophobic face of the idealized amphiphilic α-helical region. *Proc. Natl. Acad. Sci. U.S.A.* **1987**, *84*, 8340–8344.
(24) Epand, R. M.; Epand, R. F. Conformational Flexibility and Biological Activity of Salmon Calcitonin. *Biochemistry* **1986**, *25*, 1964–1968.
(25) Epand, R. M.; Epand, R. F.; Orlowski, R. C. *Biologically* active calcitonin analogs which have minimal interactions with phospholipids. *Biochem. Biophys. Res. Commun.* **1988**, *152*, 203–207.
(26) Findlay, D. M.; Michelangeli, V. P.; Orlowski, R. C.; Martin, T. J. Biological Activities and Receptor-Interactions of des-Leu16 Salmon and des-Phe16 Human Calcitonin. *Endocrinology* **1983**, *112*, 1288–1291.
(27) Basava, C.; Hostetler, K. Y. Structural determinants for the design of superpotent analogs of human calcitonin. In *Peptides: Chemistry and Biology 1991*; Smith, J. A.; Rivier, J. E., Eds.; ESCOM Science Publishers B. V.: Leiden, 1992; pp 20–22.
(28) Maier, R.; Kamber, B.; Riniker, B.; Rittel, W. Analogues of human calcitonin. IV. Influence of leucine substitutions in positions 12, 16 and 19 on hypocalcaemic activity in the rat. *Clin. Endocrinol.* **1976**, *5s*, 327s–332s.
(29) Schwartz, K. E.; Orlowski, R. C.; Marcus, R. des-Ser2 Salmon Calcitonin: A Biologically Potent Synthetic Analog. *Endocrinology* **1981**, *108*, 831–835.
(30) Epand, R. M.; Epand, R. F.; Stafford, A. R.; Orlowski, R. C. Deletion sequences of salmon calcitonin that retain the essential biological and conformational features of the intact molecule. *J. Med. Chem.* **1988**, *31*, 1595–1598.
(31) Chou, P. Y.; Fasman, G. D. Empirical predictions of protein conformation. *Annu. Rev. Biochem.* **1978**, *47*, 251–276.
(32) Azria, M. *The Calcitonins: Physiology and Pharmacology*; Karger: Basel, 1989; pp 133–143.
(33) Ösapay, G.; Profit, A.; Taylor, J. W. Synthesis of tyrocidine A: Use of oxime resin for peptide chain assembly and cyclization. *Tetrahedron Lett.* **1990**, *31*, 6121–6124.
(34) Kapurniotu, A.; Taylor, J. W. Head-to-Tail Cyclization and Use of Ca-Allyl Ester Protection Improves the Yield of Cyclic Peptides Synthesized by the Oxime Resin Method. *Tetrahedron Lett.* **1993**, *34*, 7031–7034.
(35) Mitchell, M. A.; Runge, T. A.; Mathews, W. R.; Ichhpurani, A. K.; Harn, N. K.; Dobrowolski, P. J.; Eckenrode, F. M. Problems associated with use of benzyloxymethyl protecting group for histidine. *Int. J. Pept. Protein Res.* **1990**, *36*, 350–355.
(36) Plaué, S. Synthesis of cyclic peptides on solid support. *Int. J. Pept. Protein Res.* **1990**, *35*, 510–517.
(37) Hoeger, C. A.; Kirby, D. A.; Rivier, J. E. Cysteine in peptide chemistry: Side reactions associated with and strategies for the handling of peptides containing cysteine. In *Peptides: Chemistry and Biology 1991*; Smith, J. A., Rivier, J. E., Eds.; ESCOM Science Publishers B. V.: Leiden, 1992; pp 576–577.
(38) Ferrer, M.; Woodward, C.; Barany, G. Solid-phase synthesis of bovine pancreatic trypsin inhibitor (BPTI) and two analogues. *Int. J. Pept. Protein Res.* **1992**, *40*, 194–207.
(39) Brahms, S.; Brahms, J. Determination of Protein Secondary Structure in Solution by Vacuum Ultraviolet Circular Dichroism. *J. Mol. Biol.* **1980**, *138*, 149–178.
(40) Perczel, A.; Park, K.; Fasman, G. D. Analysis of the circular dichroism spectrum of proteins using the convex constraint algorithm: a practical guide. *Anal. Biochem.* **1992**, *203*, 83–93.
(41) Doi, M.; Kobayashi, Y.; Kyogoku, Y.; Takimoto, M.; Goda, K. Structure study of human calcitonin. In *Peptides 1992: Proceedings of the 22nd European Peptide Symposium*; Schneider, C. H., Eberle, A. N., Eds.; ESCOM Science Publishers B. V.: Leiden, 1993; pp 165–167.
(42) Sönnichsen, F. D.; Van Eyk, J. E.; Hodges, R. S.; Sykes, B. D. Effect of Trifluoroethanol on Protein Secondary Structure: an NMR and CD Study Using a Synthetic Actin Peptide. *Biochemistry 1992*, *31*, 8790–8798.
(43) Arvinte, T.; Cudd, A.; Drake, A. F. Studies of human calcitonin secondary structure. In *Peptides 1992: Proceedings of the 22nd European Peptide Symposium*; Schneider, C. H., Eberle, A. N., Eds.; ESCOM Science Publishers B. V.: Leiden, 1993; pp 503–504.
(44) Fischer, J. A.; Tobler, P. H.; Kaufmann, M.; Born, W.; Henke, H.; Cooper, P. E.; Sagar, S. M.; Martin, J. B. Calcitonin: Regional distribution of the hormone and its binding sites in the human brain and pituitary. *Proc. Natl. Acad. Sci. U.S.A.* **1981**, *78*, 7801–7805.
(45) Fischer, J. A.; Sagar, S. M.; Martin, J. B. Characterization and regional distribution of calcitonin binding sites in the rat brain. *Life Sci.* **1981**, *29*, 663–671.
(46) Rizzo, A. J.; Goltzman, D. Calcitonin Receptors in the Central Nervous System of the Rat. *Endocrinology* **1981**, *108*, 1672–1677.
(47) Marx, S. J.; Woodard, C. J.; Aurbach, G. D. Calcitonin Receptors of Kidney and Bone. *Science* **1972**, *178*, 999–1000.
(48) Goltzman, D. Examination of Interspecies Differences in Renal and Skeletal Receptor Binding and Adenylate Cyclase Stimulation with Human Calcitonin. *Endocrinology* **1980**, *106*, 510–518.
(49) Kumar, M. A.; Slack, E.; Edwards, A.; Soliman, H. A.; Baghdiantz, A.; Foster, G. V.; MacIntyre, I. A. biological assay for calcitonin. *J. Endocrinol.* **1965**, *33*, 469–475.
(50) Richardson, J. S. The anatomy and taxonomy of protein structure. *Adv. Protein Chem.* **1981**, *34*, 167–339.
(51) Huwyler, R.; Born, W.; Ohnhaus, E. E.; Fischer, J. A. Plasma kinetics and urinary excretion of exogenous human and salmon calcitonin in man. *Am. J. Physiol.* **1979**, *236*, E15–E19.
(52) Burgen, A. S. V.; Roberts, G. C. K.; Feeney, J. Binding of flexible ligands to macromolecules. *Nature* **1975**, *253*, 753–755.
(53) Motta, A.; Temussi, P. A.; Wünsch, E.; Bovermann, G. A. ^{1}H NMR Study of Human Calcitonin in Solution. *Biochemistry* **1991**, *30*, 2364–2371.
(54) Byfield, P. G. H.; Clark, M. B.; Turner, K.; Foster, G. V.; MacIntyre, I. Immunochemical studies on human calcitonin M leading to information on the shape of the molecule. *Biochem. J.* **1972**, *127*, 199–206.
(55) Twery, M. J.; Seitz, P. K.; Nickols, G. A.; Copper, C. W.; Gallagher, J. P.; Orlowski, R. C. Analogue separates biological effects of salmon calcitonin on brain and renal cortical membranes. *Eur. J. Pharmacol.* **1988**, *155*, 285–292.
(56) Nakamuta, H.; Orlowski, R. C.; Epand, R. M. Evidence for Calcitonin Receptor Heterogeneity: Binding Studies with Nonhelical Analogs. *Endocrinology* **1990**, *127*, 163–169.
(57) Sexton, P. M.; Houssami, S.; Hilton, J. M.; O'Keeffe, L. M.; Center, R. J.; Gillespie, M. T.; Darcy, P.; Findlay, D. M. Identification of brain isoforms of the rat calcitonin receptor. *Mol. Endocrinol.* **1993**, *7*, 815–821.
(58) Albrandt, K.; Mull, E.; Brady, E. M. G.; Herich, J.; Moore, C. X.; Beaumont, K. Molecular cloning of two receptors from rat brain with high affinity for salmon calcitonin. *FEBS Lett.* **1993**, *325*, 225–232.
(59) Briggs, M. S.; Cornell, D. G.; Dluhy, R. A.; Gierasch, L. M. Conformation of Signal Peptides Induced By Lipids Suggest Initial Steps in Protein Export. *Science* **1986**, *233*, 206–208.
(60) Felix, A. M.; Wang, C. T.; Campbell, R. M.; Toome, V.; Fry, D.; Madison, V. S. Biologically active cyclic (lactam) analogs of growth hormone-releasing factor: Effect of ring size and location on conformation and biological activity. In *Peptides Chemistry and Biology 1991*; Smith, J. A., Rivier, J. E., Eds.; ESCOM Science Publishers B. V.: Leiden, 1992; pp 77–79.
(61) Nakamuta, H.; Furukawa, S.; Koida, M.; Yajima, H.; Orlowski, R.; Schlueter, R. Specific binding of ^{125}I-Salmon Calcitonin to rat brain: Regional variation and calcitonin specificity. *Jpn. J. Pharmacol.* **1981**, *31*, 53–60.
(62) Salomon, Y.; Londos, C.; Rodbell, M. A. Highly Sensitive Adenylate Cyclase Assay. *Anal. Biochem.* **1974**, *58*, 541–548.
(63) Altman, D. G. *Practical Statistics for Medical Research*; Chapman and Hall: New York, 1991; pp 210–214.
(64) Yates, A. J.; Guitierrez, G. E.; Garrett, I. R.; Mencel, J. J.; Nuss, G. W.; Schreiber, A. B.; Mundy, G. R. A noncyclical analog of salmon calcitonin (N$^{\alpha}$-propionyl di-Ala^{1,7}, des-Leu^{19} sCT) retains full potency without inducing anorexia in rats. *Endocrinology* **1990**, *126*, 2845–2849.

JM940573K